arXiv:1605.06386v1 [physics.soc-ph] 20 May 2016

k-core percolation on complex networks: Comparing random, localized and targeted attacks

Xin Yuan,[1] Yang Dai,[2] H. Eugene Stanley,[1] and Shlomo Havlin[1,3]
[1] *Center for Polymer Studies and Department of Physics, Boston University, Boston, Massachusetts 02215 USA*
[2] *School of Economics and Management, Southwest Jiaotong University, Chengdu 610031, China*
[3] *Minerva Center and Department of Physics, Bar-Ilan University, Ramat-Gan 52900, Israel*
(Dated: 13 May 2016)

The type of malicious attack inflicting on networks greatly influences their stability under ordinary percolation in which a node fails when it becomes disconnected from the giant component. Here we study its generalization, k-core percolation, in which a node fails when it loses connection to a threshold k number of neighbors. We study and compare analytically and by numerical simulations of k-core percolation the stability of networks under random attacks (RA), localized attacks (LA) and targeted attacks (TA), respectively. By mapping a network under LA or TA into an equivalent network under RA, we find that in both single and interdependent networks, TA exerts the greatest damage to the core structure of a network. We also find that for Erdős-Rényi (ER) networks, LA and RA exert equal damage to the core structure whereas for scale-free (SF) networks, LA exerts much more damage than RA does to the core structure.

I. INTRODUCTION

In complex networks science, malicious attacks may crucially change the structure, stability and function of a network [1–23]. The description of an attack on a network is often represented by the ordinary percolation model in which the giant connected component serves as the relevant order parameter that shows the robustness of a macroscopic cluster. The behavior of the giant connected component is characteristic of the structural transition of networks where nodes suffer either random attacks (RA) [2–4, 24–28], localized attacks (LA) [29–31] or targeted attacks (TA) [2, 3, 32, 33].

A natural generalization of ordinary percolation is the k-core percolation in which the behavior of the k-core characterizes the structural change of a network under RA [34–36]. The k-core of a network is defined as the largest subgraph in which each node has at least k neighbors and is obtained through the pruning process in which nodes of degree less than k are progressively removed. If $k = 1$, then the k-core is simply the connected component of the network and the giant k-core is the giant connected component, exactly as in ordinary percolation. If $k = 2$, we again have a continuous transition similar to ordinary percolation, as the 2-core is obtained by simply pruning all dangling branches from the 1-core [34, 37]. Under the k-core percolation with $k \geq 3$, single networks demonstrate discontinuous transitions at a k-dependent critical threshold $p_c(k)$ [34–36]. Although prior research has developed tools for probing network resilience against RA in the context of k-core percolation, and has found that degree distribution strongly influences network stability [34, 35], a systematic study of how TA and LA affect network resilience in the case of k-core percolation is still missing.

Here we extend the general formalism of the k-core percolation for uncorrelated networks with arbitrary degree distributions under RA [34, 35] to networks under LA and TA, respectively. This allows us to obtain the sizes and other structural characteristics of k-cores in a variety of damaged random networks and to compare the robustness of the networks under these three types of attack scenarios in terms of k-core percolation.

We apply our derived general frameworks to study (i) single ER networks [38, 39] with a Poisson distribution, (ii) single SF networks [8–10] with a power-law distribution, (iii) two interdependent ER networks with the same Poisson distribution in each network, and (iv) two interdependent SF networks with the same power-law distribution in each network. For each case, we investigate how the type of attack influences the k-core percolation properties. These include the size of the k-core, $M_k(p)$, as a function of p, the fraction of unremoved nodes and the critical threshold $p_c(k)$ at which the k-core $M_k(p)$ first collapses. In all cases we find that our extensive simulations and analytical calculations are in good agreement. In general, TA exerts the biggest destruction on the k-core structure of networks since the hubs of the networks−nodes with higher degrees−are more likely to be removed initially. We observe similar characteristics of robustness in both single and interdependent ER networks under both LA and RA. However, for SF networks, LA exerts considerably more damage than RA does to the core structure.

II. RA, LA AND TA ON A SINGLE NETWORK

A. Theory

(I) *Random Attack:* Following Ref. [40], we introduce the generating function of the degree distribution $P(q)$ of a random network A as

$$G_0(x) = \sum_q P(q)x^q. \quad (1)$$

After an initial attack which is manifested by the random removal of a fraction $1-p$ of nodes from the network of size N, a cascading pruning process occurs as nodes with degree less than k are progressively disconnected from the network. We denote the stage right after the random attack as stage $t = 0$ and the probability that a given end of an edge is the root of an infinite (k-1)-ary subtree as f_0 [34]. After the first round of pruning process which disconnects those nodes with active degree less than k to the rest of network, we obtain a network in which a fraction $1-p$ of nodes failed due to initial attack and some other fraction of nodes have become isolated due to k-core percolation. Now this network is at stage $t = 1$ and at this time f_0 decreases to f_1. Note an end of an edge is a root of an infinite (k-1)-ary subtree if at least $k-1$ of its children's branches are also roots of infinite (k-1)-ary subrees [34]. This leads to the equation for f_1 in terms of f_0, which is

$$f_1 = p \sum_{q=k-1}^{\infty} \frac{P(q+1)(q+1)}{\langle q \rangle} \sum_{j=k-1}^{q} C_q^j f_0^j (1-f_0)^{q-j} \equiv p\Phi(f_0), \quad (2)$$

where $C_q^j = q!/(q-j)!j!$, p is the probability that the end of the edge is occupied, $P(q+1)(q+1)/\langle q \rangle$ is the probability that a randomly chosen edge leads to a node with q out-going edges (other than the one first chosen) and $C_q^j f_0^j (1-f_0)^{q-j}$ is the probability that j out of these q branches are roots of infinite (k-1)-ary subrees. Note that j here must be at least equal to $k-1$.

Similarly, after the pruning process finishes for the second time, we would have $f_2 = p\Phi(f_1)$. More generally, at each stage t we have f_t obtained from f_{t-1} through

$$f_t = p\Phi(f_{t-1}), \quad (3)$$

and the probability that a random node in the damaged network belongs to the k-core is [34]

$$[M_k(p)]_t = p \sum_{q=k}^{\infty} P(q) \sum_{j=k}^{q} C_q^j {f_t}^j (1-f_t)^{q-j} \equiv p\Psi(f_t). \quad (4)$$

Note that $[M_k(p)]_t$ is also the normalized size of the k-core of the network at this stage. As $t \to \infty$, the network will reach a steady state and we have $f_t \to f$, with f satisfying the self-consistent equation

$$f = p\Phi(f). \quad (5)$$

Note an equivalent equation for f at the steady state was also given in Eq. (2) of Ref. [34].

We note that for any given p, f can be solved from Eq. (5) using Newton's method with a proper initial value. A trivial solution $f = 0$ exists if the occupation probability p is small and thereafter $M_k(p) = 0$, i.e., no k-core exists in this case. As p increases and at $p = p_c^{RA}(k)$, a non-trivial solution $f = f_c \neq 0$ first arises and gives birth to a k-core. This is typical first-order phase transition behavior for the network and it requires the derivatives of both sides of Eq. (5) with respect to f_c be equal [34, 35], i.e.,

$$1 = p_c^{RA}(k)\Phi^{'}(f_c). \quad (6)$$

Therefore by using Eqs. (5) and (6), the threshold of k-core percolation $p_c^{RA}(k)$ is determined by

$$p_c^{RA}(k) = 1/\Phi^{'}(f_c), \quad f_c = \Phi(f_c)/\Phi^{'}(f_c). \quad (7)$$

Here, f_c is the value of f at the birth of a k-core. When $p > p_c^{RA}(k)$, there is always a non-zero solution of f that ensures the existence of a k-core.

(II) *Localized Attack:* We next consider the localized attack on network A by the removal of a fraction $1-p$ of nodes, starting with a randomly-chosen seed node. Here we remove the seed node and its nearest neighbors, next-nearest neighbors, next-next-nearest neighbors, and continue until a fraction $1-p$ of nodes have been removed from the network. This pattern of attack reflects such real-world localized scenarios as earthquakes or the results of weapons of mass destruction. As in Ref. [29], the localized attack occurs in two stages, (i) nodes belonging to the attacked area (the seed node and the layers surrounding it) are removed but the links connecting them to the remaining nodes of the network are left in place, but then (ii) these links are also removed. Following the method introduced in Refs. [29, 41], we find the generating function for the degree distribution of the remaining network to be

$$G_{p0}(x) = \frac{1}{G_0(l)} G_0[l + \frac{G_0^{'}(l)}{G_0^{'}(1)}(x-1)], \quad (8)$$

where $l \equiv G_0^{-1}(p)$.

Next we want to find an equivalent network $\tilde{A}$ such that a random removal of a fraction $1-p$ of nodes from it will produce a network with the same degree distribution as that obtained by a LA on network A described above. We denote $P(q^{'})$ as the degree distribution of network $\tilde{A}$ and $\tilde{G}_{A0}(x)$ as its generating function. Following the argument of equivalence discussed above and by setting $\tilde{G}_{A0}(1-p+px) = G_0^p(x)$ [13, 31], and after some rearrangement, we have $\tilde{G}_{A0}(x)$ as

$$\tilde{G}_{A0}(x) = \frac{1}{G_0(l)} G_0[l + \frac{G_0^{'}(l)}{G_0^{'}(1)G_0(l)}(x-1)]. \quad (9)$$

Therefore, $P(q')$ could be generated from $\tilde{G}_{A0}(x)$ through direct differentiation [13]

$$P(q') = \frac{1}{q'!} \frac{d^{q'}}{dx^{q'}} \tilde{G}_{A0}(x). \quad (10)$$

Combining Eqs. (9) and (10) we obtain the degree distribution of the equivalent network $\tilde{A}$ as

$$P(q') = \sum_{q=q'}^{\infty} \frac{l^q}{p} P(q) C_q^{q'} (\frac{\tilde{p}}{p})^{q'} (1-\frac{\tilde{p}}{p})^{q-q'}, \quad (11)$$

with $\tilde{p} = G_0^{'}(l)/G_0^{'}(1)l$.

Thus performing k-core percolation on the resultant network after LA is equivalent to performing k-core percolation on network $\tilde{A}$ after a random removal of the same fraction of nodes. This enables us to transform a LA problem into the familiar RA problem examined in the previous scenario. Then for the LA scenario we replace $P(q)$ in Eqs. (4) and (5) with $P(q')$ obtained from Eq. (11) and obtain the size of k-core $M_k(p)$ as well as its critical threshold $p_c^{LA}(k)$.

(III) *Targeted Attack:* Next, we consider the targeted attack on network A by the removal of a fraction $1-p$ of nodes where nodes are removed based on their degree [32, 33]. This pattern of attack reflects such real-world cases as intentional attacks on important transportation hubs or sabotage on the Internet [42]. To analyze this case, a value $W_\alpha(q_i)$ is assigned to each node, which represents the probability that a node i with q_i links is initially attacked and becomes dysfunctional. This probability is described through the family of functions [43]

$$W_\alpha(q_i) = \frac{q_i^\alpha}{\sum_{i=1}^{N} q_i^\alpha}, -\infty < \alpha < +\infty. \tag{12}$$

When $\alpha > 0$, nodes with higher connectivity have a higher probability to be removed while $\alpha < 0$ indicates otherwise. Note that for $\alpha = 0$, all nodes have equal probability to be removed, which is exactly the same as the RA case.

As described in Ref. [32], the targeted attack occurs in two stages, (i) nodes are chosen according to Eq. (12) and later removed but the links connecting the removed nodes and the remaining nodes are left in place, but then (ii) these links are also removed.

Following the method introduced in Refs. [32, 41], we find the generating function for the degree distribution of the remaining network to be (only removing the nodes)

$$G_b(x) = \frac{1}{p}\sum_q P(q) l^{q^\alpha} x^q, \tag{13}$$

where $l = G_\alpha^{-1}(p)$ and $G_\alpha(x) \equiv \sum_{q=0}^{\infty} P(q) x^{q^\alpha}$. The fraction of the original links that connect to the remaining nodes is $\tilde{p} = \sum_q P(q) q l^{q^\alpha} / \sum_q P(q) q$. Further removing the links which end at the removed nodes of a randomly connected network is equivalent to randomly removing a fraction $1-\tilde{p}$ of links of the remaining nodes. Using the approach introduced in Ref. [13], we find that the generating function of the remaining nodes after the removal of the links between removed nodes and remaining nodes is

$$G_c(x) = G_b(1 - \tilde{p} + \tilde{p}x). \tag{14}$$

Next we find an equivalent network $\tilde{B}$ in which a random removal of a fraction $1-p$ of nodes will produce a network with the same degree distribution as that obtained by a TA on network A described above. We denote $P(q^{'})$ as the degree distribution of network $\tilde{B}$ and $\tilde{G}_{B0}(x)$ as its generating function. Following the equivalence argument discussed above and setting $\tilde{G}_{B0}(1-p+px) = G_c(x)$ [13], after some algebra, we obtain $\tilde{G}_{B0}(x)$ as $\tilde{G}_{B0}(x) = G_c(1+\frac{1}{p}(x-1))$. Using Eq. (14), we thus have

$$\tilde{G}_{B0}(x) = G_b(\frac{\tilde{p}}{p}(x-1)+1). \tag{15}$$

Accordingly, combining Eqs. (13) and (15) and using direct differentiation we obtain the degree distribution $P(q')$ of the equivalent network $\tilde{B}$ as

$$P(q') = \sum_{q=q'}^{\infty} \frac{l^{q^\alpha}}{p} P(q) C_q^{q'} (\frac{\tilde{p}}{p})^{q'} (1-\frac{\tilde{p}}{p})^{q-q'}. \tag{16}$$

Thus performing k-core percolation on network A after a TA is the same as performing the k-core percolation on network $\tilde{B}$ after a random removal of the same fraction of nodes. By replacing $P(q)$ in Eqs. (4) and (5) with $P(q')$ obtained from Eq. (16), for the TA scenario we can obtain the size of k-core $M_k(p)$ together with its critical threshold $p_c^{TA}(k)$.

B. Results

To test the analytical solutions derived in Section A, we conduct numerical solutions of the analytic expressions, and compare the results with simulation results on single networks with degrees following both Poisson distributions and power-law distributions under RA, LA and TA. All the simulation results are obtained for networks with $N = 10^6$ nodes.

1. Erdős-Rényi networks

We first consider ER networks of which the degree distribution is Poissonian, i.e., $P(q) = e^{-\lambda}\frac{\lambda^q}{q!}$ with the average degree denoted by λ.

In the RA scenario on an ER network with $k = 4$ and $\lambda = 10$, we exhibit in Fig. 1(a) several realizations the cascading pruning process under k-core percolation with p slightly smaller than $p_c^{RA}(k)$, in comparison with theory. Note that the simulation results for the cascading pruning agree well with analytical results from Eqs. (3) and (4). Different realizations give different results due to random fluctuations of the dynamic processes showing deviations from the mean field, rendering small fluctuations around the mean-field analytical result. To calculate the first-order phase transition point $p_c^{RA}(k)$ with good precision, as shown in Fig. 1(b), we identify the characteristic behavior of the number of iterations (NOI) in the cascading process [44]. This gives us $p_c^{RA}(k) = 0.515$, corresponding to the peak of the NOI. Figures 1(c) and 1(d) show the variation of the pruning size s_t, which is the number of nodes that are pruned at

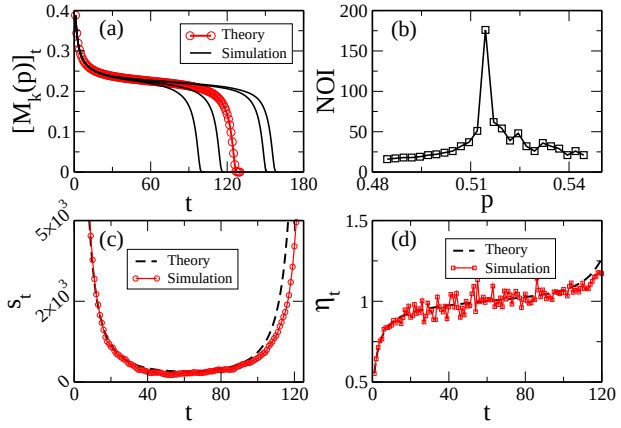


FIG. 1. (Color online) Dynamics of an ER network near criticality under random attack applying k-core percolation. (a) Dynamical process of the k-core size $[M_k(p)]_t$ of the ER network with $k = 4$, $\lambda = 10$ and $N = 10^6$ both in theory (red line with circles) and in simulation (solid black lines) at $p = 0.5145$, slightly below $p_c^{RA}(k) = 0.515$. (b) Number of iterations (NOI) before network reaching stability. This number peaks at $p = p_c^{RA}$ and it drops quickly as p moves away from $p_c^{RA}(k)$ [44, 45]. (c) At $p = 0.5145$, the red line with circles represents the variation of failure sizes s_t (only the plateau stage) for one realization in the simulation; the black dashed line shows s_t for the theoretical case. (d) At $p = 0.5145$, the red line with rectangles shows the variation of the average branching factor η_t for one realization in the simulation; the black dashed line shows η_t of the analytic solution. Note that this figure is similar to that found in interdependent networks [45].

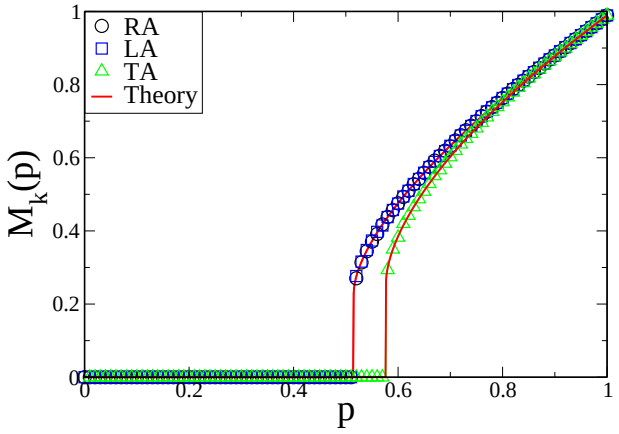


FIG. 2. (Color online) Sizes of the k-core, $M_k(p)$, as a function of the fraction of unremoved nodes, p, for a single ER network with $\lambda = 10$ and $k = 4$. Here solid lines are theoretical predictions, from Eq. (4) for RA and its counterparts of LA and TA (with $\alpha = 1$), and symbols are simulation results with network size $N = 10^6$, under RA (◯), LA (□) and TA (△). Note that for ordinary percolation under either RA or LA, the system is significantly more resilient, and the transition is continuous at $p_c = 1/\lambda = 0.1$.

stage t, and the branching factor η_t ($\eta_t = s_{t+1}/s_t$), respectively, in one typical realization that finally reached total collapse. Note that s_t initially drops as the network is still well connected and thus less nodes are pruned per pruning step ($s_t > s_{t+1}$). Then the network becomes weak enough and s_t remains at low and almost constant value during the plateau stage while the network keeps getting weaker. Finally s_t rises as a failure in the current step leads to more than one failure in the next step and results in the total collapse of the network (see Fig. 1(c)). Although s_t first decreases, the ratio of two consecutive pruning sizes, η_t, increases. Specifically η_t increases during the initial cascades from below 1 to approximately 1 (with some fluctuations) at the plateau, which starts at time T when each of the s_T pruned nodes leads, on average, to failure of another single node. This is a stable state, leading to the divergence of t for $N \to \infty$, where the cascading trees become critical branching processes [45, 46] with the average time at criticality scales as $N^{1/3}$ [45]. In a finite network of size N, however, the accumulated failures weaken the network step by step and thus s_t starts to rise, leading to the collapse of the system. During this period, η_t rises to above 1 as shown in Fig. 1(d).

When the dynamics end, the network enters the steady state. At this state, Fig. 2 shows the k-core $M_k(p)$ as a function of the occupation probability p under RA, LA and TA (with $\alpha = 1$) in the context of k-core percolation. Note that the simulation results agree well with the theoretical results and that there is first-order percolation transition behavior in all attack scenarios. Note also that $p_c^{RA}(k)$ is equal to $p_c^{LA}(k)$ and they both are smaller than $p_c^{TA}(k)$. This is similar to ordinary percolation [29, 32]. This is the case because for ER networks with $P(q) = e^{-\lambda}\frac{\lambda^q}{q!}$, from Eq. (11) the degree distribution $P(q')$ of the equivalent network $\tilde{A}$ can be calculated to be

$$\begin{aligned} P(q') &= \sum_{q=q'}^{\infty} \frac{l^q}{p} P(q) C_q^{q'} (\frac{\tilde{p}}{p})^{q'} (1-\frac{\tilde{p}}{p})^{q-q'} \\ &= \frac{e^{-\lambda}[\lambda l \frac{\tilde{p}}{p}]^{q'}}{pq'!} \sum_{q=q'}^{\infty} \frac{[\lambda l(1-\frac{\tilde{p}}{p})]^{q-q'}}{(q-q')!} \\ &= \frac{e^{-\lambda}[\lambda l \frac{\tilde{p}}{p}]^{q'}}{pq'!} e^{\lambda l(1-\frac{\tilde{p}}{p})} \\ &= e^{-\lambda}\frac{\lambda^{q'}}{q'!}, \end{aligned} \tag{17}$$

where we use $l = \frac{ln(p)}{\lambda} + 1$ and $\tilde{p} = p/l$ for simplification. Note that from Eq. (17) the degree distribution of network $\tilde{A}$ is also Poissonian and has the same average degree λ as the original network. Thus, we have $p_c^{RA}(k) = p_c^{LA}(k)$ as observed. Similarly from Eq. (16) with $\alpha = 1$, we find the degree distribution $P(q')$ of the equivalent network $\tilde{B}$ to be

$$P(q') = e^{-\lambda l^2}\frac{(\lambda l^2)^{q'}}{q'!}, \tag{18}$$

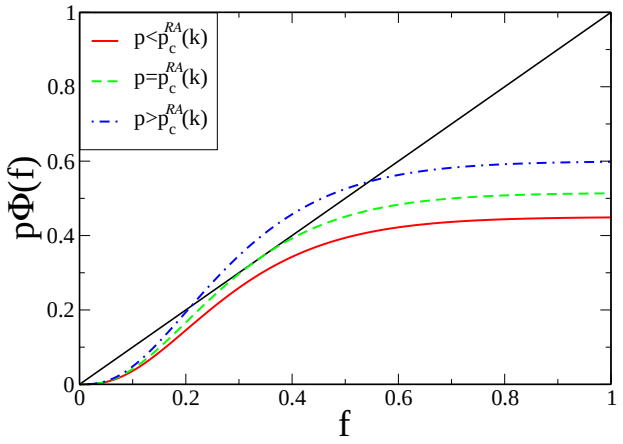


FIG. 3. (Color online) Graphical solution of Eq. (5) for the k-core percolation with $k = 4$ in an ER network under RA with an average degree of 10. The straight line and the curves $p\Phi(f)$ show, respectively, the left- and right-hand side of Eq. (5) as functions of f for different values of p. The nonzero solution of f appears above the critical value $p_c^{RA}(k) = 0.515$, at which the right-hand side curve $p\Phi(f)$ starts to intersect the straight line. The physical solution is provided by the largest root of the equation $f = p\Phi(f)$ when $p > p_c^{RA}(k)$ (the upper intersection in the plot).

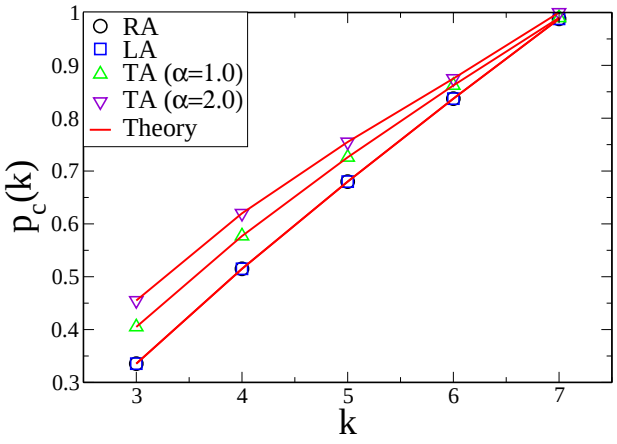


FIG. 4. (Color online) Percolation thresholds $p_c(k)$ of a single ER network as a function of k under RA, LA and TA with $\alpha = 1$, $\lambda = 10$. Here solid lines are theoretical predictions and symbols (◯ for RA, □ for LA, △ for TA with $\alpha = 1.0$ and ▽ are for TA with $\alpha = 2.0$) are simulation results with network size of $N = 10^6$ nodes. Note that LA coincides with RA.

with $l = \frac{ln(p)}{\lambda} + 1$. Note that from Eq. (18) the degree distribution of network $\tilde{B}$ is also Poissonian but has a smaller average degree λl^2 as l is always smaller than 1 [32]. Compared to that under RA, the removal of the same fraction of nodes under TA reduces a larger amount of connectivity in the network and therefore, in the context of k-core percolation, the critical threshold $p_c^{TA}(k)$ is significantly larger than $p_c^{RA}(k)$.

As an example, Fig. 3 shows the solution of Eq. (5) for different values of the occupation probability p under RA and demonstrates the origin of the first-order transition. When $p < p_c^{RA}(k)$, the straight line and the curve only have an intersection at $f = 0$, which always renders $M_k(p) = 0$ according to Eq. (4). A k-core $M_k(p)$ first arises discontinuously at $p = p_c^{RA}(k)$, when the straight line and the curve tangentially touch each other at a nonzero intersection at $f = f_c$, satisfying Eq. (6). As p increases further and becomes greater than $p_c^{RA}(k)$, $M_k(p)$ continues to exist as an additional intersection appears, and this serves as the physical solution of f (see the upper intersection in Fig. 3). Similar procedures are applied to the LA and TA scenarios as well and the corresponding $p_c^{LA}(k)$ and $p_c^{TA}(k)$ are obtained, respectively.

Next we obtain the relationship between the robustness of the network under the three types of attacks and the threshold k in the context of k-core percolation. Figure 4 shows how the percolation thresholds $p_c(k)$ under RA, LA and TA, change with k where $\lambda = 10$ for a single ER network. Here in Fig. 4, as k increases from 3 to 7, $p_c^{RA}(k)$, $p_c^{LA}(k)$ and $p_c^{TA}(k)$ increase accordingly. For each k value, $p_c^{RA}(k) = p_c^{LA}(k) < p_c^{TA}(k, \alpha = 1.0) < p_c^{TA}(k, \alpha = 2.0)$, which indicates that in the context of k-core percolation RA and LA cause the same amount of damage to the structure of an ER network, but that TA causes more severe structural damage to an ER network. Moreover, we find that RA and LA have very similar dynamic properties in terms of NOI as well as the pruning size s_t. Figure 4 also indicates that with a larger α, TA will cause more damage since higher degree nodes are more likely to be removed. Similar results are reported in the context of ordinary percolation on ER networks [29, 32].

2. *Single scale-free networks*

We next consider SF networks in which degrees of nodes follow a power law distribution, i.e., $P(q) \propto q^{-\gamma}$ with the degree exponent $\gamma \in (2, 3]$. As in Ref. [34], a size dependent cutoff $q_{cut}(N)$ of the degree distribution is introduced. For the configuration model without multiple connections the dependence $q_{cut}(N) \sim \sqrt{N}$ is usually used when $2 < \gamma \leq 3$, and first-order percolation transition behavior was observed in the RA case [34]. Figure 5 shows $M_k(p)$ as a function of the occupation probability p under RA, LA and TA (with $\alpha = 1$) under k-core percolation with $k = 4$ and $\gamma = 2.3$. The simulation results agree well with the theoretical results, and there is first-order percolation transition behavior in all attack scenarios. Note that $p_c^{LA}(k)$ is approximately equal to $p_c^{TA}(k)$, and that they both are significantly larger than $p_c^{RA}(k)$. Because SF networks are ultrasmall [10, 47], the LA process can easily spread from the seed node to high degree hubs in several steps and therefore severely disrupts the core structure of the network, an outcome similar to that of the TA process. This is in marked contrast to the case of ER networks in which the majority of

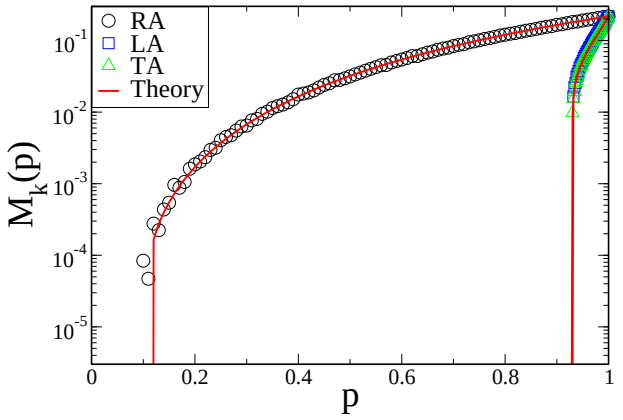


FIG. 5. (Color online) Sizes of the k-core, $M_k(p)$, as a function of the fraction of unremoved nodes, p, for a single SF network with $\gamma = 2.3$, $q_{min} = 2$, $q_{cut}(N) = 1000$ and $k = 4$. Here solid lines are theoretical predictions, from Eq. (4) for RA and its counterparts of LA and TA (with $\alpha = 1$), and symbols are simulation results with network size $N = 10^6$, under RA (◯), LA

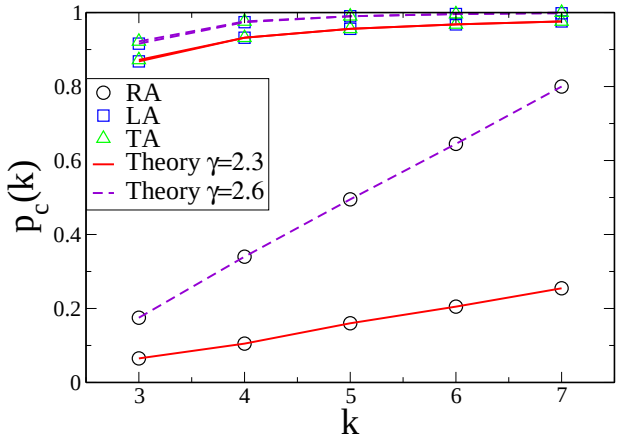


FIG. 6. (Color online) Percolation thresholds $p_c(k)$ of a single SF network as a function of k under RA, LA and TA with $\alpha = 1$, $q_{min} = 2$, $q_{cut}(N) = 1000$ for $\gamma = 2.3$ (solid red lines) and $\gamma = 2.6$ (dashed purple lines). Here lines are theoretical predictions and symbols (◯ for RA, □ for LA and △ are for TA) are simulation results with network size of $N = 10^6$ nodes.

nodes have degrees around the average degree and therefore for the RA and LA processes, nodes of high degrees are less likely to be reached than those in the TA process.

Next we determine the relationship between the robustness of the network under three types of attacks and the threshold k in the context of k-core percolation. For a single SF network, Fig. 6 shows how the percolation thresholds $p_c(k)$ under RA, LA and TA (with $\alpha = 1$) change with k for two values of γ. As seen in Fig. 6, the $p_c(k)$ values under all attack scenarios for $\gamma = 2.3$ are smaller than those for $\gamma = 2.6$, which indicates that SF networks with smaller γ values are more stable in the context of k-core percolation. In addition, for each value of γ as k increases from 3 to 7, $p_c^{RA}(k)$, $p_c^{LA}(k)$ and $p_c^{TA}(k)$ increase accordingly. For each k value, $p_c^{LA}(k) \approx p_c^{TA}(k) > p_c^{RA}(k)$, which indicates that in the context of k-core percolation, LA and TA (with $\alpha = 1$) exert approximately the same amount of damage to the structure of a SF network whereas RA produces less severe structural damage to a SF network. Analogous results are reported in the context of ordinary percolation on SF networks [29, 32].

III. RA, LA AND TA ON INTERDEPENDENT NETWORKS

A. Theory

We extend the formalism of ordinary percolation on fully interdependent networks introduced in Ref. [24] to k-core percolation. Specifically, we consider two networks A and B with the same number of nodes N. Within each network the nodes are randomly connected with the same degree distribution $P(q)$. A fraction d_A of nodes from network A depend on nodes in network B, and a fraction d_B of nodes from network B depend on nodes in network A. We also assume that if a node i in network A depends on a node j in network B and node j depends on node l in network A, then $l = i$, which rules out the feedback condition [48]. This interdependence means that if node i in network A fails, its dependent node j in network B will also fail, and vice versa.

(I) *Random Attack*: We begin by randomly removing a fraction $1 - p$ of nodes in network A. All the nodes in network B that are dependent on the removed nodes in network A are also removed. Then a cascading pruning process begins, and nodes with degree less than k_1 in network A and k_2 in network B are sequentially removed in the k-core percolation process. Due to interdependence, the removal process iterates back and forth between the two networks until they fragment completely or produce a mutually connected **k**-core with no further disintegration, where $\mathbf{k} \equiv (k_1, k_2)$ [24, 36].

When the system of interdependent networks stops disintegrating, as in a single network we let $f_A(f_B)$ be the probability that a given end of an edge of network $A(B)$ is the root of an infinite ($k_{1(2)}$-1)-ary subtree. An end of an edge is a root of an infinite (k_1-1)-ary subtree of network A if it is an autonomous node [49] and at least $k_1 - 1$ of its children's branches are also roots of infinite (k_1-1)-ary subrees; otherwise, despite that, the node it depends on has to be in the k_2-core of network B. Similar arguments exist for edges in network B. These lead to the equation of f_A in terms of f_A and f_B as

$$\begin{aligned} f_A &= p\Phi_A(f_A)(1 - d_A) + p\Phi_A(f_A)\Psi_B(f_B)d_A \\ &= p\Phi_A(f_A)\left[(1 - d_A) + d_A\Psi_B(f_B)\right], \end{aligned} \tag{19}$$

where p is the probability that an end n_0 of an edge is occupied, $\Phi_A(f_A)$ is the probability that n_0 is a root of an infinite (k_1-1)-ary subtree, $1 - d_A$ is the probability

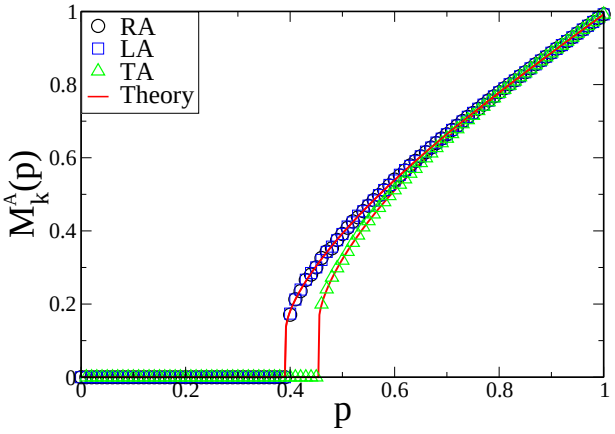


FIG. 7. (Color online) Sizes of k-core of network A, $M_{\mathbf{k}}^A(p)$, as a function of the fraction of unremoved nodes, p, for two partially interdependent ER networks with $d = 0.5$, $\lambda = 10$ and $\mathbf{k} = (3, 4)$. Here solid red lines are theoretical predictions, from Eq. (21) for RA and its counterparts of LA and TA for $\alpha = 1$, and symbols are simulation results with network size $N = 10^6$, under RA (◯), LA (□) and TA (△).

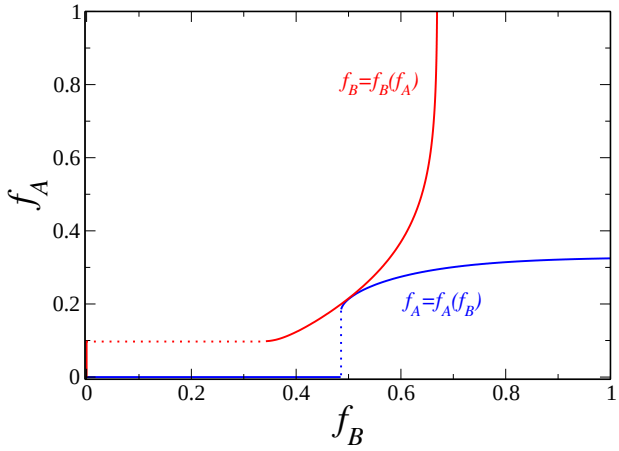


FIG. 8. (Color online) Graphical solution of Eqs. (19) and Eq. (20) for the k-core percolation with $\mathbf{k} = (3, 4)$ and $d = 0.5$ in two interdependent ER networks A and B with the average degree 10, where network A is damaged initially under RA. The blue and red curves show, respectively, Eq. (19) and Eq. (20) for the value of $p = p_c^{RA}(\mathbf{k})$. The nontrivial solution of f_A and f_B appears at the critical value $p_c^{RA}(\mathbf{k}) = 0.391$, at which the two curves intersect tangentially with each other, satisfying Eq. (22). When $p > p_c^{RA}(\mathbf{k})$, these two curves will always have a nonzero intersection and it serves as the p

that n_0 is an autonomous node, d_A is the probability that n_0 depends on a node n' in network B, and $\Psi_B(f_B)$ is the probability that n' is in the k_2-core of network B. Following similar arguments, we obtain the equation of f_B in terms of f_A and f_B,

$$f_B = \Phi_B(f_B)\left[(1 - d_B) + d_B p \Psi_A(f_A)\right]. \qquad (20)$$

Note that for any given value of p, f_A and f_B can be solved from Eqs. (19) and (20) using Newton's method after choosing appropriate initial values. We denote $M_{\mathbf{k}}^A(p)$ and $M_{\mathbf{k}}^B(p)$ as the probability that a randomly chosen node in network A and B belongs to the mutually connected $\mathbf{k}$-core, respectively, and they satisfy

$$\begin{cases} M_{\mathbf{k}}^A(p) = p\Psi_A(f_A)\left[1 - d_A + d_A\Psi_B(f_B)\right], \\ M_{\mathbf{k}}^B(p) = \Psi_B(f_B)\left[1 - d_B + d_B p\Psi_A(f_A)\right]. \end{cases} \qquad (21)$$

Note that the mutually connected $\mathbf{k}$-core is made up of the k_1-core in network A (with its normalized size denoted by $M_{\mathbf{k}}^A(p)$) and the k_2-core in network B (with its normalized size denoted by $M_{\mathbf{k}}^B(p)$).

The trivial solution $f_A = f_B = 0$ for low occupation probability p signifies the absence of a $\mathbf{k}$-core in the system. As p increases, a nontrivial solution emerges in the critical case ($p = p_c^{RA}(\mathbf{k})$) in which two curves $f_A = f_A(f_B)$ and $f_B = f_B(f_A)$ tangentially touch each other, i.e.,

$$\frac{df_A}{df_B} \cdot \frac{df_B}{df_A} = 1 \qquad (22)$$

which, together with Eqs. (19) and (20), gives the solution for $p_c^{RA}(\mathbf{k})$ and the critical size of the mutually connected $\mathbf{k}$-core. When $p > p_c^{RA}(\mathbf{k})$, these two curves

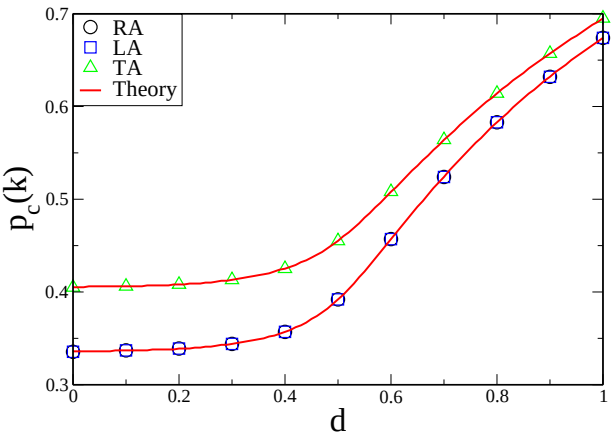


FIG. 9. (Color online) Percolation thresholds $p_c(\mathbf{k})$ of two interdependent ER networks as a function of interdependence strength d under RA, LA and TA with $\lambda = 10$ and $\mathbf{k} = (3, 4)$. Here solid lines are theoretical predictions and symbols (◯ for RA, □ for LA and △ are for TA) are simulation results with network size of $N = 10^6$ nodes. Note that for $d = 0$ the results reduce to the case of single networks with $k = 3$, shown in Fig. 4.

will always have a nonzero intersection that constitutes a physical solution. For simplicity and without loss of generality, we use $d_A = d_B \equiv d$ throughout the rest of this paper.

(II) *Localized Attack*: When LA is performed on the system of interdependent networks A and B described above, we find an equivalent random network E with a

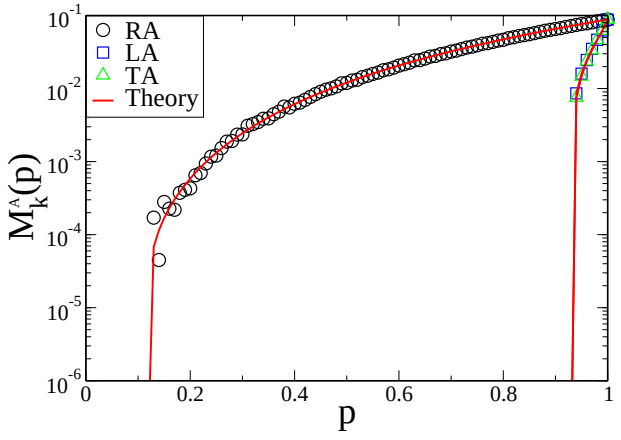


FIG. 10. (Color online) Sizes of the k-core of network A, $M_{\mathbf{k}}^A(p)$, as a function of the fraction of unremoved nodes, p, for two partially interdependent SF networks with $d = 0.5$, $\gamma = 2.3$, $q_{min} = 2$, $q_{cut}(N) = 1000$ and $\mathbf{k} = (3, 4)$. Here solid lines are theoretical predictions, from Eq. (21) for RA and its counterparts of LA and TA for $\alpha = 1$, and symbols are simulation results with network size $N = 10^6$, under RA (◯), LA (□) and TA (△).

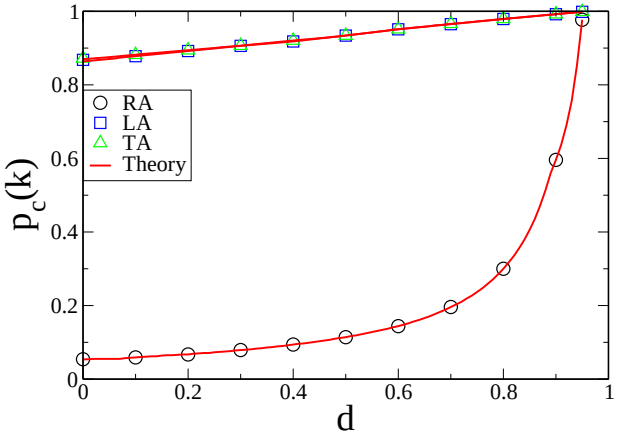


FIG. 11. (Color online) Percolation thresholds $p_c(\mathbf{k})$ of two interdependent SF networks as a function of interdependence strength d under RA, LA and TA with $\alpha = 1$, $q_{min} = 2$, $q_{cut}(N) = 1000$, $\gamma = 2.3$ and $\mathbf{k} = (3, 4)$. Here solid lines are theoretical predictions and symbols (◯ for RA, □ for LA and △ are for TA) are simulation results with network size of $N = 10^6$ nodes. Note that for d=0 the results reduce to the case of single networks with k=3, seen in Fig. 6.

degree distribution $P(q')$ [from Eq. (11)] such that after a random attack in which a fraction $1-p$ of nodes in network E are removed, the degree distribution of the remaining network is the same as the degree distribution of the remaining network resulting from an LA on network A. Then by mapping the LA problem on interdependent networks A and B to a RA problem on a transformed pair of interdependent networks E and B, we can apply the mechanism of RA on interdependent networks to solve $p_c^{LA}(\mathbf{k})$ and the mutually connected $\mathbf{k}$-core under LA.

(III) *Targeted Attack*: Analogously, when TA is performed on the interdependent networks A and B described above, we find an equivalent random network F with a degree distribution $P(q')$ [from Eq. (16)] such that after a random attack in which a fraction $1-p$ of nodes in network F are removed, the degree distribution of the remaining network is the same as the degree distribution of the remaining network resulting from an TA on network A. Thus, by mapping the TA problem on interdependent networks A and B to a RA problem on a transformed pair of interdependent networks F and B, we can apply the mechanism of RA on interdependent networks to solve $p_c^{TA}(\mathbf{k})$ and the mutually connected $\mathbf{k}$-core under TA in the case of k-core percolation.

B. Results

1. *Two interdependent Erdős-Rényi networks*

We start with two partially interdependent networks in which the degrees both follow the same Poisson distribution and exert a RA on network A, initiating a k-core percolation pruning process that continues until equilibrium is reached. We then follow the same procedure with the same set-up but this time using a LA and TA to initiate the pruning process. Figure 7 shows the k-core $M_{\mathbf{k}}^A(p)$ of network A as a function of the occupation probability p under RA, LA and TA (with $\alpha = 1$) in the context of k-core percolation with $d = 0.5$, $\mathbf{k} = (3, 4)$ and $\lambda = 10$. The simulation results agree well with the theoretical results, and there are first-order percolation transitions in all attack scenarios. As in single ER networks, note that $p_c^{RA}(\mathbf{k})$ is equal to $p_c^{LA}(\mathbf{k})$ and both are smaller than $p_c^{TA}(\mathbf{k})$.

Figure 8 shows for instance the critical solution of Eqs. (19) and (20) for the case of RA shown in Fig. 7. When $p < p_c^{RA}(\mathbf{k})$, the two curves representing Eqs. (19) and (20) correspondingly intersect only at the origin, and this always renders a zero-sized k-core $M_{\mathbf{k}}^A(p)$ according to Eq. (21). A k-core $M_{\mathbf{k}}^A(p)$ first arises discontinuously at $p = p_c^{RA}(\mathbf{k})$, when these two curves tangentially touch each other at a nonzero intersection at (f_{A_c}, f_{B_c}), satisfying Eq. (22). As p increases further above $p_c^{RA}(\mathbf{k})$, $M_{\mathbf{k}}^A(p)$ continues to exist because of the presence of a nonzero intersection that serves as the nontrivial solution of Eqs. (19) and (20). Similar procedures are applied to the LA and TA scenarios as well and the corresponding $p_c^{LA}(\mathbf{k})$ and $p_c^{TA}(\mathbf{k})$ are obtained, respectively.

Next we obtain the relationship between the robustness of the network system, i.e., the threshold $p_c(\mathbf{k})$, under three types of attacks and the interdependence strength d in the context of k-core percolation. Figure 9 shows how the percolation thresholds $p_c(\mathbf{k})$ under RA, LA and TA (with $\alpha = 1$), change with d where $\mathbf{k} = (3, 4)$ and $\lambda = 10$ for two ER networks. As seen in Fig. 9, when

d increases from 0 to 1, $p_c^{RA}(\mathbf{k})$, $p_c^{LA}(\mathbf{k})$ and $p_c^{TA}(\mathbf{k})$ increase accordingly, which means that the higher the level of interdependence between networks A and B, the less resilient they are against attacks. Note that $d = 0$ corresponds to the case in which there is no interdependence between networks A and B and the thresholds $p_c(\mathbf{k})$ reduce to those shown in Fig. 4 at $k = 3$. For each d value, $p_c^{RA}(\mathbf{k}) = p_c^{LA}(\mathbf{k}) < p_c^{TA}(\mathbf{k})$, which indicates that in the context of k-core percolation, RA and LA exert the same level of damage to the structure of an ER network, but that TA produces more severe damage to an ER network. Similar results are reported in the context of ordinary percolation on interdependent ER networks [31, 32].

2. *Two interdependent scale-free networks*

We construct two interdependent networks in which the degrees in each follow the same power law distribution. Figure 10 shows the k-core $M_{\mathbf{k}}^A(p)$ of network A as a function of the occupation probability p under RA, LA and TA (with $\alpha = 1$) under k-core percolation with $\mathbf{k} = (3, 4)$ and $\gamma = 2.3$. The simulation results agree well with the theoretical results, and there is first-order percolation transition behavior in all attack scenarios. Note that $p_c^{LA}(\mathbf{k})$ is approximately equal to $p_c^{TA}(\mathbf{k})$ and they both are significantly larger than $p_c^{RA}(\mathbf{k})$. As in single SF networks, the LA process can easily spread from the seed node to high degree hubs in few steps and therefore greatly disintegrates the core structure of the network, similar to the TA process. This is in strong contrast to the case of ER networks in which most nodes have degrees close to the average degree and therefore for the RA and LA processes, nodes of high degrees are less likely to be removed compared to the TA process.

Next we compare the robustness of the network system under each of the three types of attacks as a function of the interdependence strength d in the context of k-core percolation. Figure 11 shows how the percolation thresholds $p_c(\mathbf{k})$ under RA, LA and TA (with $\alpha = 1$), change with d where $\mathbf{k} = (3, 4)$ and $\gamma = 2.3$ for two SF networks. Here in Fig. 11, as d increases from 0 to 1, $p_c^{RA}(\mathbf{k})$, $p_c^{LA}(\mathbf{k})$ and $p_c^{TA}(\mathbf{k})$ increase accordingly, which means that the more interdependent networks A ad B are on each other, the less resilient they will be against attacks. Note that the $d = 0$ case corresponds to the scenario shown in Fig. 6 at $k = 3$. For each d value, $p_c^{LA}(\mathbf{k}) \approx p_c^{TA}(\mathbf{k}) > p_c^{RA}(\mathbf{k})$, which indicates that in the context of k-core percolation, LA and TA (with $\alpha = 1$) exert approximately the same level of damage to the structure of a SF network whereas RA produces less severe damage to a SF network. Similar results are reported in the context of ordinary percolation on SF networks [29, 32].

IV. CONCLUSIONS

We have studied and compared the robustness of both single and interdependent networks under three types of attacks in the context of k-core percolation. We show that interdependence between networks makes the system more vulnerable than their single network counterparts. In addition, we map a network under LA and TA into an equivalent network under RA, solve analytically the k-core percolation problem, and show how the initial attack type affects the robustness of networks. In general, TA exerts the most damage. In particular, LA and RA cause equal damage to ER networks whereas in ultrasmall networks like SF networks, LA causes much more damage than RA does. These findings hold for both single networks and interdependent networks.

ACKNOWLEDGMENTS

We wish to thank DTRA, NSF, the European MULTIPLEX, ONR, and the Israel Science Foundation for financial support. Y.D. acknowledges support from the NSFC (Grant No. 71201132) and the DFME (Grant No. 20120184120025).

[1] D. J. Watts and S. H. Strogatz, Nature **393**, 440 (1998).
[2] R. Albert, H. Jeong, and A.-L. Barabási, Nature **406**, 378 (2000).
[3] R. Cohen, K. Erez, D. Ben-Avraham, and S. Havlin, Phys. Rev. Lett. **85**, 4626 (2000).
[4] D. S. Callaway, M. E. J. Newman, S. H. Strogatz, and D. J. Watts, Phys. Rev. Lett. **85**, 5468 (2000).
[5] R. Albert and A.-L. Barabási, Rev. Mod. Phys. **74**, 47 (2002).
[6] M. E. Newman, SIAM Rev. **45**, 167 (2003).
[7] C. Song, S. Havlin, and H. A. Makse, Nature **433**, 392 (2005).
[8] A.-L. Barabási and R. Albert, Science **286**, 509 (1999).
[9] G. Caldarelli and A. Vespignani, *Large scale structure and dynamics of complex networks: from information technology to finance and natural science*, vol. 2 (World Scientific, 2007).
[10] R. Cohen and S. Havlin, *Complex networks: structure, robustness and function* (Cambridge University Press, 2010).
[11] V. Rosato et al., Int. J. Crit. Infrastruct. **4**, 63 (2008).
[12] A. Arenas, A. Díaz-Guilera, J. Kurths, Y. Moreno, and C. Zhou, Phys. Rep. **469**, 93 (2008).
[13] M. Newman, *Networks: An Introduction* (Oxford University Press, 2010).
[14] G. Li, S. D. S. Reis, A. A. Moreira, S. Havlin, H. E. Stanley, and J. S. Andrade, Phys. Rev. Lett. **104**, 018701 (2010).
[15] C. M. Schneider et al., Proc. Natl. Acad. Sci. **108**, 3838 (2011).

[16] A. Bashan et al., Nat. Commun. **3**, 702 (2012).
[17] S. Dorogovtsev and J. Mendes, *Evolution of networks: From biological nets to the Internet and WWW* (Oxford University Press, 2013).
[18] J. Ludescher et al., Proc. Natl. Acad. Sci. **110**, 11742 (2013).
[19] X. Yan, Y. Fan, Z. Di, S. Havlin, and J. Wu, PLOS ONE **8**, e69745 (2013).
[20] S. Boccaletti et al., Phys. Rep. **544**, 1 (2014).
[21] D. Li et al., Proc. Natl. Acad. Sci. **112**, 669 (2015).
[22] F. Radicchi, Nat. Phys. **11**, 597 (2015).
[23] F. Morone and H. A. Makse, Nature **524**, 65 (2015).
[24] S. V. Buldyrev, R. Parshani, G. Paul, H. E. Stanley, and S. Havlin, Nature **464**, 1025 (2010).
[25] T. P. Peixoto and S. Bornholdt, Phys. Rev. Lett. **109**, 118703 (2012).
[26] G. J. Baxter, S. N. Dorogovtsev, A. V. Goltsev, and J. F. F. Mendes, Phys. Rev. Lett. **109**, 248701 (2012).
[27] A. Bashan, Y. Berezin, S. V. Buldyrev, and S. Havlin, Nat. Phys. **9**, 667 (2013).
[28] F. Radicchi and A. Arenas, Nat. Phys. **9**, 717 (2013).
[29] S. Shao, X. Huang, H. E. Stanley, and S. Havlin, New J. Phys. **17**, 023049 (2015).
[30] Y. Berezin, A. Bashan, M. M. Danziger, D. Li, and S. Havlin, Sci. Rep. **5**, 8934 (2015).
[31] X. Yuan, S. Shao, H. E. Stanley, and S. Havlin, Phys. Rev. E **92**, 032122 (2015).
[32] X. Huang, J. Gao, S. V. Buldyrev, S. Havlin, and H. E. Stanley, Phys. Rev. E **83**, 065101 (2011).
[33] G. Dong, J. Gao, L. Tian, R. Du, and Y. He, Phys. Rev. E **85**, 016112 (2012).
[34] S. N. Dorogovtsev, A. V. Goltsev, and J. F. F. Mendes, Phys. Rev. Lett. **96**, 040601 (2006).
[35] A. V. Goltsev, S. N. Dorogovtsev, and J. F. F. Mendes, Phys. Rev. E **73**, 056101 (2006).
[36] N. Azimi-Tafreshi, J. Gómez-Gardeñes, and S. N. Dorogovtsev, Phys. Rev. E **90**, 032816 (2014).
[37] G. J. Baxter, S. N. Dorogovtsev, A. V. Goltsev, and J. F. F. Mendes, Phys. Rev. E **83**, 051134 (2011).
[38] P. Erdős and A. Rényi, Publ. Math. Debrecen **6**, 290 (1959).
[39] B. Bollobás, *Random graphs* (Springer, 1998).
[40] M. E. J. Newman, Phys. Rev. E **66**, 016128 (2002).
[41] J. Shao, S. V. Buldyrev, L. A. Braunstein, S. Havlin, and H. E. Stanley, Phys. Rev. E **80**, 036105 (2009).
[42] R. Cohen, K. Erez, D. ben Avraham, and S. Havlin, Phys. Rev. Lett. **86**, 3682 (2001).
[43] L. K. Gallos, R. Cohen, P. Argyrakis, A. Bunde, and S. Havlin, Phys. Rev. Lett. **94**, 188701 (2005).
[44] R. Parshani, S. V. Buldyrev, and S. Havlin, Proc. Natl. Acad. Sci. **108**, 1007 (2011).
[45] D. Zhou, A. Bashan, R. Cohen, Y. Berezin, N. Shnerb, and S. Havlin, Phys. Rev. E **90**, 012803 (2014).
[46] G. J. Baxter, S. N. Dorogovtsev, K.-E. Lee, J. F. F. Mendes, and A. V. Goltsev, Phys. Rev. X **5**, 031017 (2015).
[47] R. Cohen and S. Havlin, Phys. Rev. Lett. **90**, 058701 (2003).
[48] J. Gao, S. V. Buldyrev, H. E. Stanley, X. Xu, and S. Havlin, Phys. Rev. E **88**, 062816 (2013).
[49] R. Parshani, S. V. Buldyrev, and S. Havlin, Phys. Rev. Lett. **105**, 048701 (2010).